Plant Soil (2025) 517:985–1003
https://doi.org/10.1007/s11104-025-07911-8

RESEARCH ARTICLE

How provenance and cultivation method shape morphological and physiological traits in the nickel hyperaccumulator *Odontarrhena chalcidica*

Benedetta Montanarini · Mirko Salinitro · Maria Roberta Randi · Davide Cavalletti · Stefania Monari · Guillaume Echevarria · Annalisa Tassoni

Received: 13 May 2025 / Accepted: 10 September 2025 / Published online: 26 September 2025

Abstract

Background and aims Nickel is economically important, but its mining is energy-intensive and environmentally damaging. Agromining, which employs hyperaccumulator plants, represents a sustainable alternative. *Odontarrhena chalcidica* (Brassicaceae) shows a Ni uptake potential promising for agromining. This study aimed at assessing morphological and physiological traits and Ni content of four *O. chalcidica* genotypes from Northern Greece. For the first time, a multidimensional approach was used to compare plant traits and Ni accumulation of different genotypes across various cultivation systems.

Methods Genotypes were phenotyped for morphological and physiological traits. Nickel accumulation in roots, stems, and leaves was quantified. Plants were grown in aeroponics, hydroponics and pot systems to assess trait consistency. Morphological traits were evaluated through biometric measurements and Environmental Scanning Electron Microscopy. Physiological photosynthetic parameters were analysed and chlorophyll content determined. Nickel content was quantified using monochromatic X-Ray Fluorescence spectroscopy.

Results Significant phenotypic variability was observed among genotypes. Morphological parameters, such as stomatal and trichome densities, showed stability across cultivation conditions. Hydroponics and aeroponics proved to be suitable for phenotyping, as they did not significantly alter key morphological and physiological traits observed in pot. However, biomass yield and Ni uptake varied across cultivation system for both roots and leaves, with hydroponics being optimal for growth and Ni accumulation.

Responsible Editor: Paula Pongrac.

Benedetta Montanarini and Mirko Salinitro contributed equally to this work.

Supplementary Information The online version contains supplementary material available at https://doi.org/10.1007/s11104-025-07911-8.

B. Montanarini · D. Cavalletti · S. Monari · A. Tassoni (✉)
Department of Biological Geological and Environmental Sciences, University of Bologna, Via Irnerio N.42, 40126 Bologna, Italy
e-mail: annalisa.tassoni2@unibo.it

M. Salinitro
Laboratory of Plant Genetics, University of Wageningen, Droevendaalsesteeg N. 2 Pb , 6708 Wageningen, Netherlands

M. R. Randi
Department of Biological Geological and Environmental Sciences, University of Bologna, Via Selmi N.3, 40126 Bologna, Italy

G. Echevarria
Botanickel, Rue De Sarrebourg N.14, 54300 Luneville, France

Conclusions The phenotypic diversity observed among genotypes proved to remain consistent across cultivation systems. *Odontarrhena chalcidica* traits observed in hydroponics and aeroponics are correlated with those observed in pot, thus could be the basis for future field agromining applications.

Keywords Aeroponics · Agromining · Hydroponics · Nickel · Phytomining · Plant phenotyping

Introduction

Nickel (Ni) is a transition metal widely distributed along the Earth's crust, usually in combination with oxygen and sulphur (Genchi et al. 2020). Nowadays, due to its physical and chemical properties, Ni is a key element for industrial and technological processes from aerospace and engine systems to chemical, medical and environmental applications, to energy and metal processing industries (Mankins and Lamb 1990). In particular, Ni role in stainless steel production and composition of lithium-ion batteries (LIBs) electric vehicles (EVs) is fundamental (Winjobi et al. 2022). The demand for LIBs has increased dramatically in the past decades and is expected to grow more in the future as consequence of the European Union policies that push the transition to clean energy and reduced greenhouse gas emissions. Nickel based products are not only a valuable alternative for reducing carbon emissions, but they also have the potential to mitigate environmental impact by lowering energy consumption (Mistry et al. 2016).

Traditional nickel extraction is energy-intensive and location-dependent, involving the preconcentration of laterite and sulphide ores or recycling Ni-rich waste. This process includes pyrometallurgical and hydrometallurgical methods that emit significant greenhouse gases (GHG) (Meshram et al. 2019; Mistry et al. 2016). Additionally, these methods contribute to deforestation and biodiversity loss, undermining ecosystem carbon sequestration (Paulikas et al. 2020).

An alternative to traditional Ni-ore mining is agromining (Kidd et al. 2018), an established method that exploits the ability of plants to extract metals from soil and concentrate them in their biomass. Agromining can be considered innovative since the growing of plants requires less energy, therefore leading to lower GHG emission, compared to traditional extraction (van der Ent et al. 2018). Lastly, it may exploit marginal or degraded lands, improving soil quality and promoting biodiversity (Chaney and Baklanov 2017).

According to their ability to tolerate metals present in the soil, plants can be grouped into three categories: excluders, indicators and hyperaccumulators (Baker 1981; Corzo Remigio et al. 2020). Hyperaccumulators can absorb high amounts of elements from the soil and concentrate them in their aboveground tissues (Corzo Remigio et al. 2020), having Bioaccumulation Factor (BAF: shoot to soil ratio) and Translocation Factor (TF: shoot to root ratio) (Burkhard 2021; Pachura et al. 2016) higher than 1. In addition, hyperaccumulator are also defined based on absolute metal concentration in their shoot. Thresholds have been fixed for several trace metals (Reeves et al. 2018), for nickel is equal to 1,000 µg of Ni per g of dry weight (DW) in their shoots without exhibiting toxicity (Baker and Brooks 1989; Jaffré et al. 1976). Examples of other metals and their respective thresholds are: cadmium (Cd) 100 µg g^{-1}, zinc (Zn) 3000 µg g^{-1}, cobalt (Co) and copper (Cu) at 300 µg g^{-1} (Krzciuk and Gałuszka 2015; van der Ent et al. 2019).

Among remarkable hyperaccumulators in temperate regions, *Noccaea caerulescens* (J.Presl & C.Presl) F.K.Mey., found in scattered locations across Europe from Spain to Poland, is renowned for its ability to accumulate zinc, reaching concentrations of up to 15,000 µg g^{-1} (Assunção et al. 2003). Another relevant hyperaccumulator is *Odontarrhena chalcidica* (Janka) Španiel, Al-Shehbaz, D.A.German & Marhold a species from the Brassicaceae family, native to the Balkan region, ranging from Bosnia and Herzegovina to Turkey (Bettarini et al. 2021).

This species has already been integrated into the agromining economy due to its ability to accumulate up to 22,400 µg g DW^{-1} of Ni (Rosenkranz et al. 2019). A recent study demonstrated how soil fertilization can influence Ni uptake in this species, with Ni accumulation ranging from 14,000 to 18,500 µg Ni g DW^{-1}, depending on the soil treatment, and a maximum yield of 166.5 kg Ni ha^{-1} (Bani et al. 2024). This species shows strong potential for agromining for several reasons. First, it meets the biomass yield and nickel uptake requirements critical for the agromining

industry. Second, its adaptation to the Mediterranean climate makes it particularly suitable for European applications, offering a viable option for local nickel production. This species exhibits considerable variation in plant architecture, size, developmental patterns, and leaf morphology, both at the population and individual levels (Cecchi et al. 2018). Classified as Chamaephyte, this semi-woody plant typically exhibits a biennial life cycle. The plant is a much-branched subshrub with suberect, woody-at-base stems that flowers in the second year before setting seeds. It has bushy growth. The leaves are alternate, long up to 4 cm with shapes from almost round to ovate usually pointed at the apex. Moreover, they can be from deep green to grey colour depending on trichome density (Cecchi et al. 2020). Because of its great natural genetic variability, this species can potentially be improved through the selection of desired traits, following the application of targeted breeding.

The aims of the present study are: (i) determining the phenotypic variation among individuals coming from four different genotypes of *O. chalcidica* originating from ultramafic regions of West Macedonia and Epirus (Greece) by assessing morphological traits (plant architecture, specific leaf area, total leaf area, biomass, stomata and trichomes density), physiological traits (assimilation rate, transpiration rate, stomatal conductance and chlorophyll content) and Ni accumulation in roots, stems and leaves; (ii) defining the consistency of the above cited plant traits typical of each genotype, among individuals grown in three different cultivation regimes (pot, hydroponic and aeroponic system). The results will pave the way to understanding whether *O. chalcidica* traits are preserved and comparable among different growing systems. This will unveil the possibility of carrying out future studies of plant phenotyping and breeding (including speed breeding) under controlled conditions, such as hydroponics and aeroponics, significantly shortening plant cycles in view of extended and sustainable agromining processes.

Materials and methods

Germplasm collection

Bulk seeds of *Odontarrhena chalcidica* (Brassicaceae family) were collected from four sites across West Macedonia and Epirus (Greece) (Fig. 1). Sites were either ultramafic (for genotypes EX, AO and KT) or non-ultramafic (for genotype GR) and from two different altitudes above sea level (a.s.l.) (lower a.s.l.: GR 615 m, EX 675 m, AO 650 m; higher a.s.l. KT 1683 m). Seeds were germinated on sand to obtain 20–50 plants per population. Subsequently, one individual plant per population was randomly selected after one year. Each selected individual was propagated via cuttings, and the resulting clones ($n = 12$) were used in the trial. Cuttings rooted after 2 weeks in an aeroponic system, and after were transferred to the proper system for acclimatation period (day 0). All cuttings survived after transfer and acclimatation.

The extended names of the study sites and their corresponding geographic coordinates will not be disclosed in this publication, based on an agreement of confidentiality among the partners.

Cultivation regimes and nickel bioavailability

Sixteen plants ($n = 4$ for each genotype), were grown in each cultivation system: aeroponic, hydroponic and pot. Environmental conditions were fixed across all systems, as the trial was conducted simultaneously in the same greenhouse under a 16 h light/8 h dark photoperiod, Light intensity of 500 (µmol m^2s^{-1}) PAR, and temperature ranging between 25 and 15 °C during day and night, respectively. The duration of the study was 6 weeks (Fig. 2).

The nutrient solution provided to the hydroponic and aeroponic systems was a commercial nutrient solution CANNA Aqua Vega Classic (CANNA International NV, Bruxelles, Belgium) used at half-strength, spiked with 50 µM of Ni and with pH adjusted at 6.5. The half-strength nutrient solution contained the following concentrations (in mg L^{-1}): 0.002 Fe chelated with diethylenetriaminepentaacetic acid (Fe–DTPA), 0.003 Fe chelated with ethylenediamine-N,N'-bis(2-hydroxyphenylacetic acid) (Fe–EDDHA), 5.645 K, 5.200 N, 0.567 P, 0.784 Mg, 1.644 Ca, 1.041 S, 0.011 B, 0.001 Cu, 0.021 Mn, 0.003 Mo, and 0.011 Zn.

To minimise variations hydroponic and aeroponic systems shared a common nutrient solution tank and recirculation system. The same nutrient solution was also applied for watering the pot plants but diluted 1:1 with distilled water. The 1 L pots were filled with serpentinites soil collected at the ultramafic site of Mt.

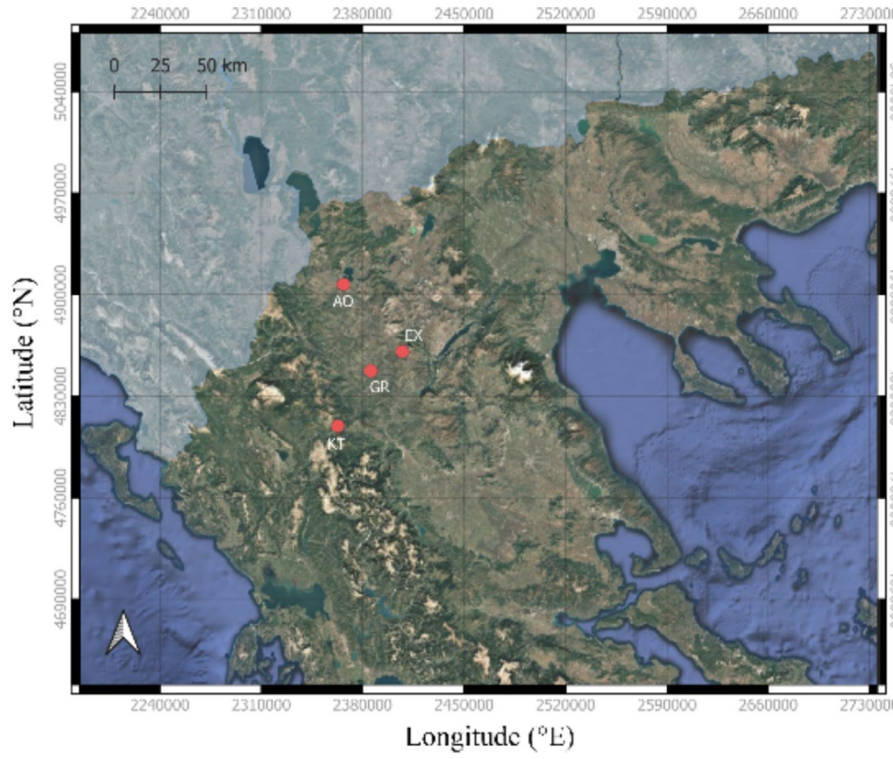

Fig. 1 Map of the sampling sites in West Macedonia and Epirus (Greece). Red dots represent accession sites EX, AO, KT and GR. Map generated using QGis v. 3.34 (QGIS Development Team 2022). Coordinates shown in WGS84 (EPSG:4326)

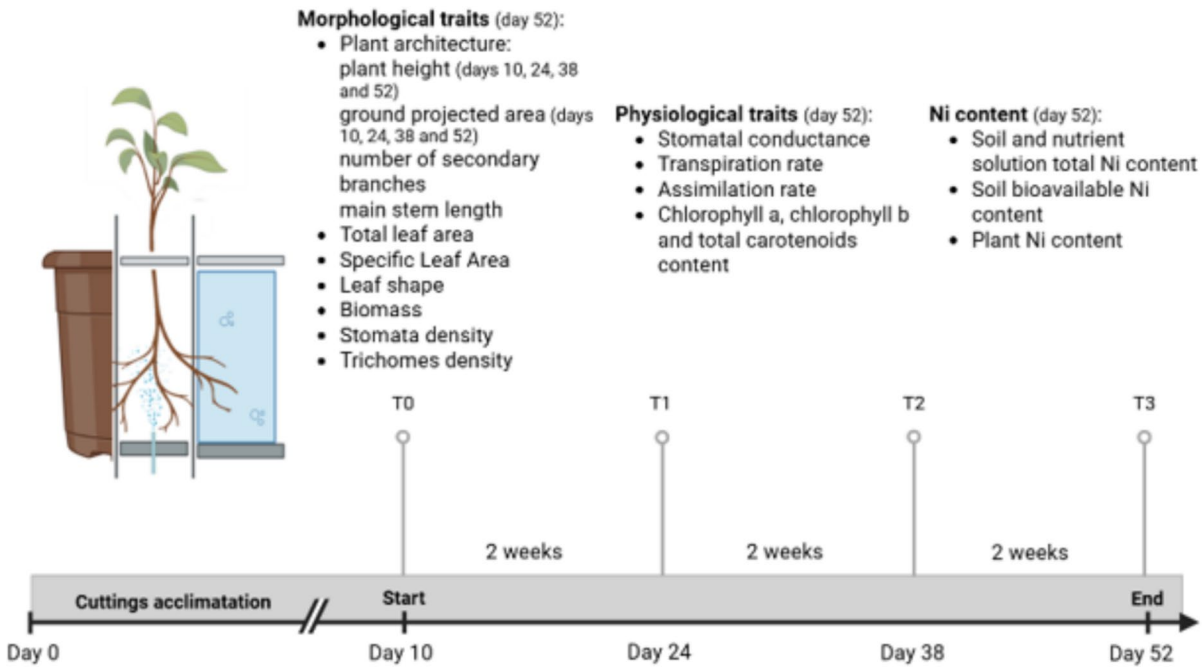

Fig. 2 Overview of the greenhouse experiment, including the sampling timeline and the parameters assessed at their respective time points. Image created in https://BioRender.com

Prinzera (Parma, Italy), after sieving it with a 2 cm mesh cutoff.

Nickel content was determined in nutrient solution (hydroponic and aeroponic) (day 10, 24, 38, 52), and in soil (pot system, day 0) along the plant growing period. Soil samples ($n=5$) from Mt. Prinzera were analysed to determine both total and bioavailable Ni content (day 0). The samples were air-dried in a dehydrating oven at 40 °C until constant weight and then sieved through a 2 mm mesh. For total Ni determination (µg g DW^{-1}), 0.5 g DW of each dried and sieved subsample was placed into custom-made XRF sample holders and sealed with a 6 µm polypropylene thin film. The samples were analysed using a Z-spec instrument, monochromatic X-Ray Fluorescence (XRF) spectroscopy (Z-SPEC JP-500, East Greenbush, NY, USA), set to *soil* mode. Bioavailable Ni content was assessed by diethylenetriaminepentaacetic acid (DTPA) extraction (Lindsay and Norvell 1978). For each sample, 0.6 g DW of soil was extracted with 1.2 mL of DTPA extraction solution in 2 mL centrifuge tubes. The DTPA extraction solution was prepared by dissolving 14.92 g L^{-1} triethanolamine (TEA), 1.47 g L^{-1} $CaCl_2{\cdot}2H_2O$, and 1.97 g L^{-1} DTPA in Milli-Q water, and adjusting the pH to 7.3 with HCl. Samples were shaken for 2 h, then centrifuged at 10,000 rpm for 3 min. A 0.5 mL aliquot of the supernatant was transferred to a new tube and diluted to 2 mL with Milli-Q water. Samples were analysed using the Z-spec in *water* mode and results expressed as mg L^{-1}. Nickel concentration (mg L^{-1}) in the nutrient solution of both aeroponic and hydroponic systems was measured by XRF in triplicate at each time point (days 10, 24, 38, and 52), using 3 mL aliquots.

Plant morphological traits

To assess plant morphological differences several parameters were measured: plant height, ground projecting area, length of the main stem, number of secondary branches, total leaf area, Specific Leaf Area (SLA), leaf shape, biomass, trichomes and stomata densities. The first four traits listed constitute the subset following reported as 'plant architecture'.

The height and the ground projecting area were evaluated for each individual plant every two weeks (day 10, 24, 38 and 52). Pictures were taken with a digital photograph system (12 MP, f/1.8), ensuring a white background and a scale in the frame, to calculate the area or length of interest with ImageJ software (Schneider et al., 2012) (https://imagej.net/ij/index.html). The length of the main stem as well as the number of secondary branches were measured at the end of the study (day 52) to enhance the information regarding the spatial development of the plants.

The total leaf area (mm^2) was measured at the end of the study (day 52) using ImageJ software. For each plant, all leaves were carefully removed from the stems and placed on a white paper background, where they were photographed from a top-down view. The images were then analysed using the *Analyze Particles* function in ImageJ, and the areas of all leaves were summed to obtain the total leaf area. This parameter is crucial as it directly influences the plant's photosynthetic capacity, affecting its overall growth and metal uptake efficiency.

The Specific Leaf Area (SLA) (mm^2 mg DW^{-1}), which indicates leaf area available for light absorption and photosynthesis in relation to its biomass, was determined at the end of the study (day 52) by calculating the ratio between leaf area (mm^2, assessed by ImageJ) and leaf dry weight (mg DW).

The leaf shape was evaluated by analysing the circularity (Schindelin et al. 2012) of leaves ($n=5$) per individual at the end of the study (day 52). For this analysis the *Circularity* command on the ImageJ software was used and the following equation applied:

$$\text{Circularity} = \frac{4\pi \times \text{Leaf Area}}{(\text{Leaf perimeter})^2}$$

Results can range from 0 to 1, where 1 describes a perfect circle.

At the end of the six-week study (day 52), the biomass of each plant was assessed by separating every individual into roots, stems, and leaves, which were then weighted individually. Samples were briefly rinsed, if necessary, with deionized water to remove soil particles and then air-dried. Following, the samples were oven-dried for 16 h at 40 °C until constant weight (g DW).

Trichomes and stomata densities (number mm^{-2}) were examined (day 52) on both abaxial and adaxial surfaces of the leaf with an electron microscope ESEM (Environmental Scanning Electron Microscopy) FEG (Field Emission Gun) Thermoscientific

Quattro S (Thermo Fisher Scientific, Waltham, Massachusetts, USA) (Fig. 3). The following operative conditions were applied: acceleration potential of 10 kV, 0.32nA beam current and working distance between 9 and 11 mm. Leaf samples (5 mm^2) were oven-dried at 40 °C overnight before being layered with the gold coat with a sputter coater (Biorad SC 502, Hercules, California, USA). Three leaves per each individual plant were scanned for ESEM image acquisition.

Physiological traits

To evaluate plant photosynthetic efficiency, transpiration rate (mol H_2O m^{-2} s^{-1} – GasEx E), assimilation rate (µmol CO_2 m^{-2} s^{-1} – GasEx A) and stomatal conductance (mol H_2O m^{-2} s^{-1}— GasEx gsw) were measured using a LI-6400 infrared gas analyzer (LI-COR, Lincoln, Nebraska, USA) equipped with a light emitting diode (LED) source and an external photosynthetic photon flux density (PPFD) sensor. For each plant, measurements were performed on three leaves selected from the middle section of the stem. The obtained values were referred to the abaxial/adaxial stomatal density ratio observed for each genotype.

The content of chlorophyll a (Chl a), chlorophyll b (Chl b) and total carotenoids were spectrophotometrically determined (Radwan et al. 2007). Fresh leaves were stored at −80° until analysis. Frozen samples were homogenized with liquid nitrogen, and 100 mg fresh weight (FW) of each was added with 0.75 mL of 85% (v/v) acetone for photosynthetic pigments extraction. The extract was mixed twice for 30 s and centrifugated at 4 °C, 2500 rpm for 5 min. The supernatant was analysed with a Cary 60 UV–Vis spectrophotometer (Agilent Technologies, Santa Clara, CA, USA) at three wavelengths (663 nm, 644 nm and 452.5 nm) for the concentration determination (mg g FW^{-1}) by using the following equations:

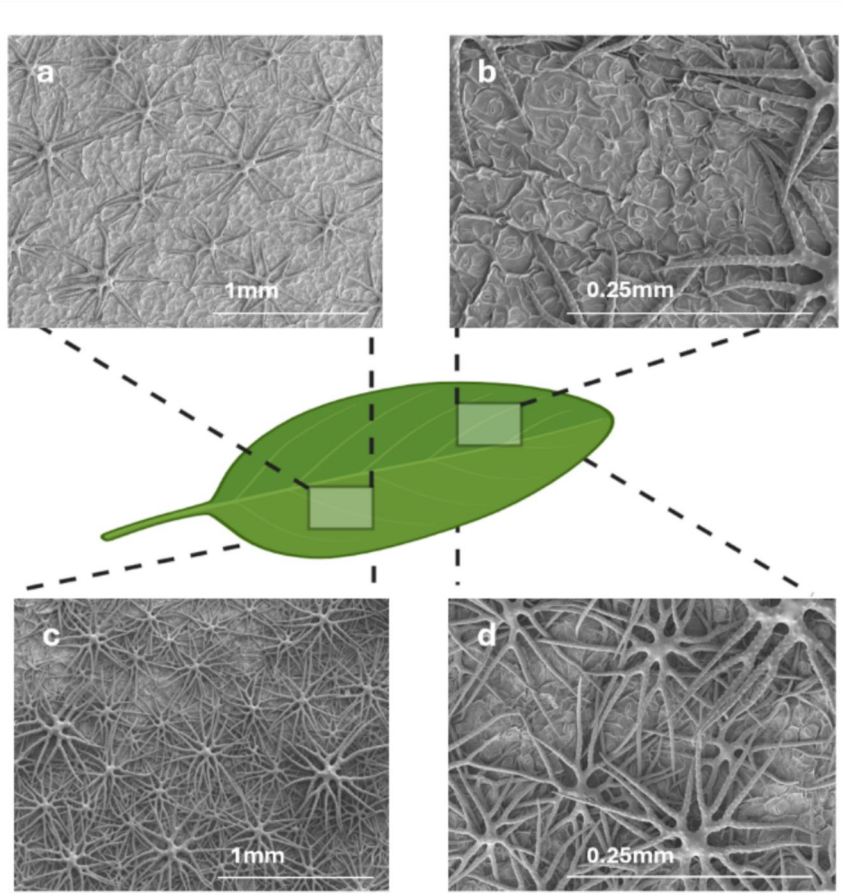

Fig. 3 Example of ESEM images of different magnification (150X for **a, c**; 400X for **b, d**) showing trichomes and stomata of both pages of a leaf. **(a, b)** Adaxial page, **(c, d)** abaxial page

$$Chlorophyll\ a\ =\ 10.3\ \times\ Abs_{663}\ -\ 0.098\ \times\ Abs_{664} \qquad Chlorophyll\ b\ =\ 19.7\ \times\ Abs_{644}\ -3.87\ \times\ Abs_{643}$$

$$Carotenoids\ =\ 4.2\ \times\ Abs_{452.5}\ -\ [(0.0264\ \times\ chl\ a)\ +\ (0.426\ \times\ chl\ b)]$$

Concentrations of nickel in plant material

Nickel content was assessed both in plant aerial parts (stem and leaves) and in roots, separately. Data were also used to calculate the plant Translocation Factor (TF, shoot metal concentration/root metal concentration) (Krzciuk and Gałuszka 2015). This parameter indicates the plant's ability to transport elements from the root to the aerial parts. In hyperaccumulators, TF values are typically greater than 1, and higher TF values reflect greater efficiency in metal translocation.

The nickel content (µg g DW^{-1}) was analysed in all samples using monochromatic X-Ray Fluorescence (XRF) spectroscopy (Z-SPEC JP-500, East Greenbush, NY, USA). Powdered dry plant tissue samples (0.4–0.6 g DW) were placed into the custom XRF sample holder and covered with a thin film (12 µm) of polypropylene and measured for 30 s using a monochromatic excitation beam in Z-spec *plant* mode.

Statistical Analyses

Graphical and statistical analyses were conducted utilizing R version 4.1.2 (R Core Team 2023) and Microsoft Excel© for Microsoft 365. All data were tested for homogeneity of variance by using Levene's test implemented in the *car* package (Fox and Weisberg 2019) (https://www.john-fox.ca/Companion/). The normality of the variables was determined using the Shapiro–Wilk normality test (function *Shapiro.test()* in base R). Parametric data underwent analysis of variance (ANOVA) (function *aov()* in base R) followed by Tukey HSD post-hoc test (function *TukeyHSD()* in base R) to evaluate differences among compared groups ($p < 0.05$). Non-parametric variables were assessed with the Kruskal–Wallis Rank Sum test (function *kruskal.test()* in base R) followed by Dunn's multiple pairwise comparison post-hoc test ($p < 0.05$) performed using the *dunn.test* package (Dinno 2024) (https://CRAN.R-project.org/package=dunn.test). Differences were evaluated: (i) by comparing the same genotype across the three cultivation systems to assess the effect of the cultivation method, and (ii) by comparing different genotypes within each cultivation system.

No combined factorial model, including both genotype and cultivation system factors, was used. Specifically, all plants were randomly positioned inside each system, within the greenhouse and cultivated under identical environmental conditions.

Results

Cultivation regimes and nickel bioavailability

Sixteen plants ($n = 4$ for each genotype) of *Odontarrhena chalcidica*, were grown in three different cultivation systems, aeroponic, hydroponic and pot, for 52 days. To evaluate whether the nickel content was comparable across the three cultivation systems, its content was measured in nutrient solution (day 10, 24, 38, 52) used both for aeroponic and hydroponic setup and as a bioavailable fraction (DTPA-extractable Ni) in pot system in soil originating from Mt. Prinzera (day 0) (Table S1). The total nickel concentration in Mt. Prinzera soil samples was 1047.38 µg g DW^{-1}, as determined by X-ray fluorescence (XRF) analysis. The bioavailable Ni fraction was 5.90 mg L^{-1} (corresponding to 9.83 µg g DW^{-1}), representing approximately 0.94% (w/w) of the total Ni content. This low proportion reflects the limited availability of Ni for plant uptake despite the high total concentration typical of serpentinic soils. The Ni concentration in the nutrient solution of both hydroponic and aeroponic systems averaged 1.42 mg L^{-1} throughout the experimental period. This value is of the same order of magnitude to the DTPA-extractable Ni observed in the soil used in the pot experiment (Table S1).

Morphological traits

Plant architecture (Fig. 4) was described by four traits. Number of secondary branches and main stem length were measured at the end of the study (day 52) while ground projected area and plant

height data were recorded every two weeks (days 10, 24, 38 and 52).

The number of secondary branches (Fig. 4a) was stable among genotypes, with individuals grown in the hydroponic system always displaying the highest number in all genotypes (EX: 40.50; AO: 21.00; KT: 37.75; GR: 43.24). Statistically significant differences were present in the EX and GR genotypes among plants grown in aeroponic and pot compared to those in hydroponic ($p < 0.05$), with values exceeding 40 in hydroponics and below 20 in both aeroponics and pot systems. For the KT genotype, a significant difference was found between aeroponics and hydroponics ($p < 0.01$), with mean values of 10.00 and 37.75, respectively. AO genotype, on the other hand, did not display significant variation at different cultivation regimes.

The main stem length (Fig. 4b) showed differences among genotypes, but no significant variation regarding cultivation regimes. Genotypes EX and GR had no statistical difference in stem length in all cultivation systems (EX: aeroponic 374.7 mm, hydroponic 372.4 mm, pot 309.9 mm; GR; aeroponic 329.5 mm, hydroponic 364.5 mm, pot 264.5 mm), while they significantly differed respect to AO genotype ($p < 0.01$) (AO; aeroponic 171.3 mm, hydroponic 167.0 mm, pot 143.0 mm). In particular, the EX genotype showed the longest main stem, with an average of 352.0 mm in all systems.

Ground projected area (Fig. 4c) displayed a trend comparable to the number of secondary branches. Almost all genotypes across all cultivation systems were similar, except for EX and GR grown in

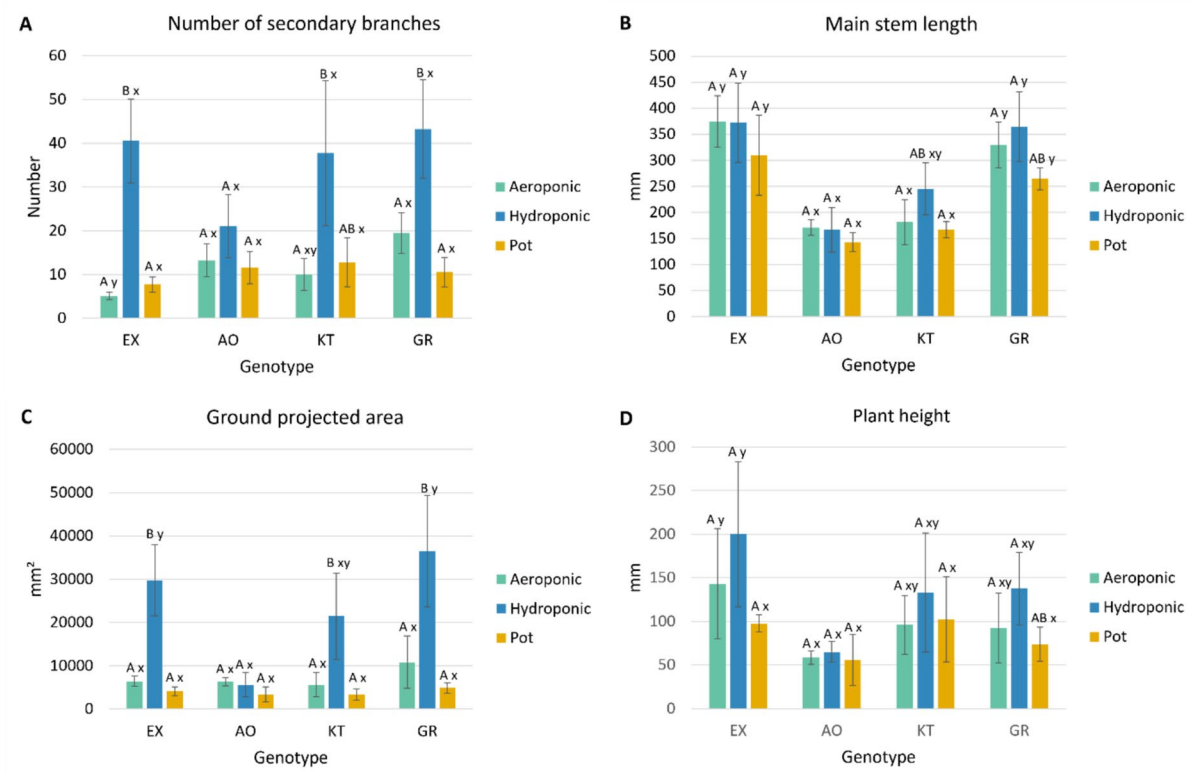

Fig. 4 Plant architecture traits of four genotypes of *Odontarrhena chalcidica* in aeroponic, hydroponic and pot cultivation regimes (day 52): (**a**) number of secondary branches, (**b**) main stem length, (**c**) ground projected area, (**d**) plant height. Upper case letters and lowercase letters indicate statistically significant differences among cultivation systems within the same genotype and among different genotypes in the same cultivation system and were evaluated by the ANOVA/Kruskal–Wallis tests followed by Tukey HSD/Dunn's tests ($p < 0.05$). Data are given as mean ($n = 4$) ± SD

hydroponics, which showed widest areas of 29,800 mm^2 and 36,400 mm^2 on average, respectively.

Plant height (Fig. 4d) was similar for each genotype in all cultivation systems. No statistical differences were notable within this morphological trait across different growing conditions, with the exception of EX and AO genotypes in hydroponics showing in the second a 67.45% lower height (200.01 mm and 65.09 mm respectively) ($p < 0.05$).

Plant architecture was overall affected by the cultivation system, in particular by the hydroponic regimes which displayed individuals with the highest performances across all traits and genotypes (Fig. S1). The only exception was the ground projected area of AO, being higher in the aeroponic system (630 mm^2) compared to the hydroponic one (570 mm^2) (Fig. 4c). Genotypes GR and KT displayed quite homogenous plant architecture, being both plant height and ground projected area 106 mm and 13,800 mm^2 on average in all cultivation systems. Genotype EX grew morphologically as a bush, with a long main stem (374.0 mm in hydroponic and 375.0 mm in aeroponic) but with a relatively limited plant height (200 mm in hydroponic and 143 mm in aeroponic). Even if it is the highest genotype present, part of the main stem laid on the ground before developing upwards. Lastly, the AO genotype had a stunted spatial development, since all four traits of the plant architecture displayed lower values.

The total leaf area (mm^2) (day 52) displayed no significant differences among genotypes; however, significant differences were found among cultivation systems within the same genotype (Fig. 5). Genotypes GR and KT displayed a similar pattern in the different cultivation systems, reaching the largest leaf area in the hydroponic system (averages of 71,500 mm^2 and 87,700 mm^2, respectively). Individuals from EX reached a high total leaf area in the hydroponic and pot regimes (49,000 mm^2 and 60,200 mm^2, respectively), while individuals in the aeroponic system (6924.12 mm^2) were significantly lower ($p < 0.05$). The area was uniform only in the AO genotype with an average of 15,914.32 mm^2 on average in all three systems.

Specific Leaf Area (SLA) unveils the potential relative growth rate of a plant or the mass-based maximum photosynthetic rate. Higher SLA reflects a larger leaf area per unit of dry mass, facilitating more efficient light interception and CO_2 assimilation. This efficiency supports faster biomass accumulation and overall plant productivity. The values (Table S2), collected at the end of the study (day 52), were consistent within genotypes and systems, having an average of 11.80 mm^2 mg DW^{-1} and reaching the highest levels in the hydroponic system for KT genotype (14.44 mm^2 mg DW^{-1}, Table S2). Plants belonging to the AO genotype grown in pot (8.68 mm^2 mg DW^{-1}) regime differed statistically from those grown under

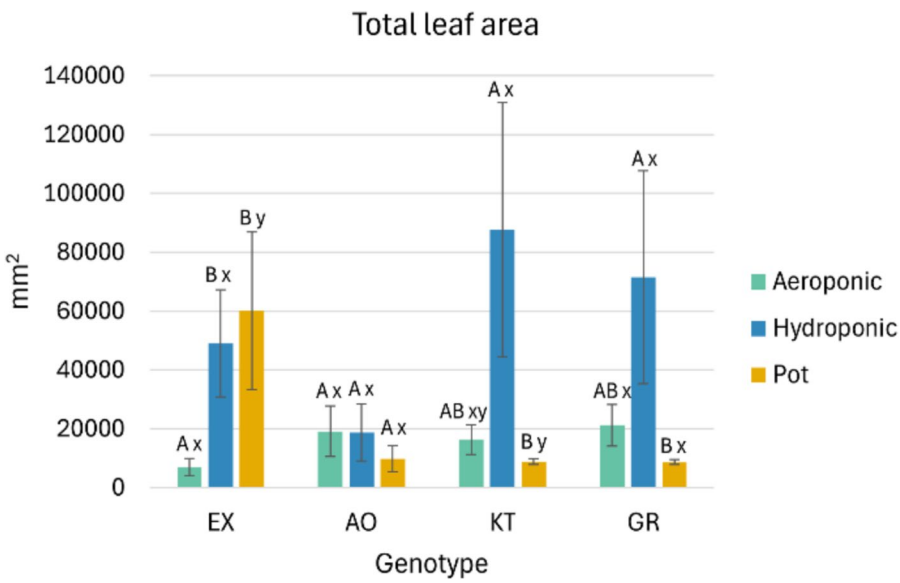

Fig. 5 Total leaf area (mm^2) of the four genotypes of *Odontarrhena chalcidica* in aeroponic, hydroponic and pot cultivation regimes. Upper case letters and lowercase letters indicate statistically significant differences among cultivation systems within the same genotype and among different genotypes in the same cultivation system and were evaluated by the ANOVA/Kruskal–Wallis tests followed by Tukey HSD/Dunn's tests ($p < 0.05$). Data are given as mean ($n = 4$) ± SD

aeroponics or hydroponic (12.02 mm^2 mg DW^{-1} and 11.35 mm^2 mg DW^{-1} respectively) ($p < 0.05$).

The leaf shape, measured with the *circularity* command on the ImageJ software, was uniform within genotypes across aeroponics, hydroponics and pot cultivation, indicating that the growing system did not influence the leaf shape, but each genotype displayed its own phenotype (Fig. 6). KT plants statistically strongly differed from the other genotypes ($p < 0.001$) in all the cultivation regimes having an average circularity of 0.75. All genotypes had leaves with smooth margins and reticulate venation, while they differed in size and shape. Leaves from KT genotype tended to be obovoid in shape, while those from GR and EX were predominantly elliptical and ovate, respectively. Genotype AO differed the most from the others, exhibiting smaller dimensions and a notably hairier surface and texture.

Roots, stems, and leaves dry weight was measured per each individual plant (Fig. 7). Across all genotypes and growing systems, leaves consistently exhibited the highest biomass compared to roots and stems. The GR genotype demonstrated the best performance, particularly in the hydroponic system, with an average leaf biomass of 6.97 g DW. Conversely, the AO genotype exhibited the lowest biomass, especially in the pot system, where leaves, roots and stems reached only 0.72 g DW, 0.55 g DW and 0.26 g DW (Fig. 7a-c), respectively. All four genotypes performed best under hydroponic conditions, with the sole exception of AO, which showed no significant differences across cultivation regimes. Focusing on leaves biomasses, enhanced performances were observed in the hydroponic system compared to the others. Genotypes EX, GR, and KT showed increases of 536%, 258% and 359%, respectively, compared to those observed in aeroponic system (Fig. 7a).

Stomata and trichome densities were evaluated on both abaxial and adaxial surfaces of the leaves. Stomata density was similar among genotypes (Table S3), and few significant differences were detected across cultivation systems: GR and KT (165.40 mm^{-2} and 166.35 mm^{-2}, respectively) plants differed statistically ($p < 0.05$) from AO and EX (100.06 mm^{-2} and 95.01 mm^{-2}, respectively) for the stomata number on the adaxial surface in the hydroponic system, having lower numbers. The KT genotype grown in pot displayed the overall highest number of stomata in both abaxial and adaxial surfaces (472.22 mm^{-2} and 167.30 mm^{-2}, respectively).

Trichome density displayed a pattern similar to stomata (Table S4). The number of trichomes per

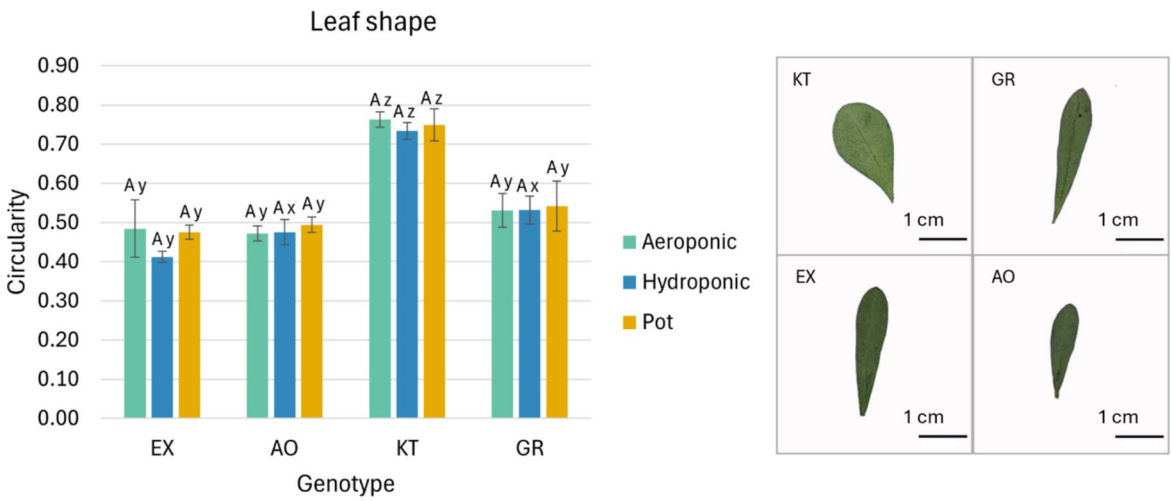

Fig. 6 Analysis of leaf shape of the four genotypes of *Odontarrhena chalcidica* in hydroponic and pot cultivation regimes. Upper case letters and lowercase letters indicate statistically significant differences among cultivation systems within the same genotype and among different genotypes in the same cultivation system and were evaluated by the ANOVA/Kruskal–Wallis tests followed by Tukey HSD/Dunn's tests ($p < 0.05$). Data are given as mean ($n = 4$) ± SD. The leaf photos are representative for each genotype and were taken by B. Montanarini

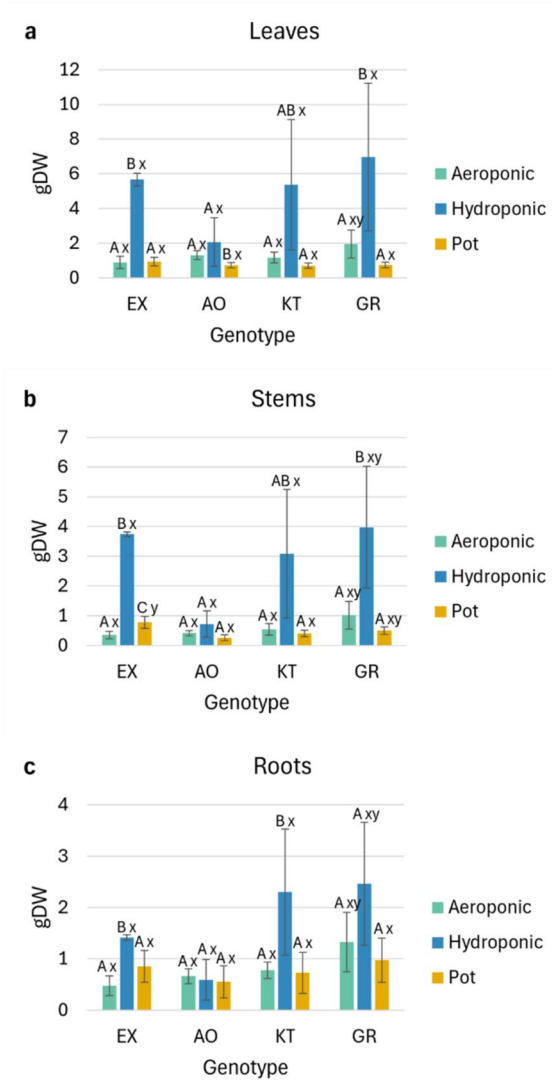

Fig. 7 Leaves (**a**), stems (**b**) and roots (**c**) biomass (g DW per plant) of the four genotypes of *Odontarrhena chalcidica* in aeroponic, hydroponic and pot cultivation regimes. Upper case letters and lowercase letters indicate statistically significant differences among cultivation systems within the same genotype and among different genotypes in the same cultivation system and were evaluated by the ANOVA/Kruskal–Wallis tests followed by Tukey HSD/Dunn's tests ($p < 0.05$). Data are given as mean ($n = 4$) ± SD

mm^2 on the adaxial surface in the hydroponic system showed a statistically significant difference among genotypes ($p < 0.001$). EX and GR displayed similar values (on average 9.96 mm^{-2}), while AO and KT differed markedly with averages of 19.52 and 4.53 trichomes per mm^2, respectively.

Physiological traits

Photosynthetic parameters (transpiration rate, assimilation rate and stomatal conductance) and chlorophyll content were assessed at day 52 to evaluate the impact of the cultivation system on the overall physiological efficiency of the genotypes and to detect potential stress conditions in plants (Tables S5 and S6).

Parameters related to leaf gas exchanges showed few significant differences among genotypes and cultivation regimes (Table S5). Specifically, the transpiration rate (GasEx E) of EX plants within the aeroponic system displayed a significantly higher average ($p < 0.05$) (0.014 mol H_2O m^{-2} s^{-1}), respect the other genotypes (overall average 0.011 mol H_2O m^{-2} s^{-1}). For assimilation rate (GasEx A) measurements ranged from a minimum of 17.711 µmol CO_2 m^{-2} s^{-1} in EX (pot) to a maximum of 26.994 µmol CO_2 m^{-2} s^{-1} in AO (pot). Regarding stomatal conductance (GasEx gsw), the lowest efficiency was detected in the GR genotype grown in pot (on average 0.480 mol H_2O m^{-2} s^{-1}), while the highest values were recorded for EX genotype in the aeroponic system (on average 0.915 mol H_2O m^{-2} s^{-1}).

The content of chlorophyll a (Chl a), chlorophyll b (Chl b), and carotenoids was measured by spectrophotometric analysis (Table S6). No significant variations were detected in the Chl a content, except for the EX plants that showed a slightly higher concentration in the aeroponics (37.13 mg g FW^{-1}) compared to other samples (on average of 30.61 mg g FW^{-1}). The cultivation regimes did not cause significant changes in the overall Chl a content for the AO, GR, and KT genotypes, while significant variation ($p < 0.001$) was detected for the EX individuals grown in different systems (Table S6). No significant Chl b and carotenoid content variations were observed across all genotypes and cultivation systems. Notably, the EX plants grown in hydroponics system exhibited the lowest levels of photosynthetic pigments: Chl a (15.43 mg g FW^{-1}), Chl b (7.60 mg g FW^{-1}), and carotenoids (3.29 mg g FW^{-1}).

Nickel content

Nickel was determined (day 52) in roots, stems and leaves of each individual plant of the four genotypes across all the experimental conditions (Fig. 8).

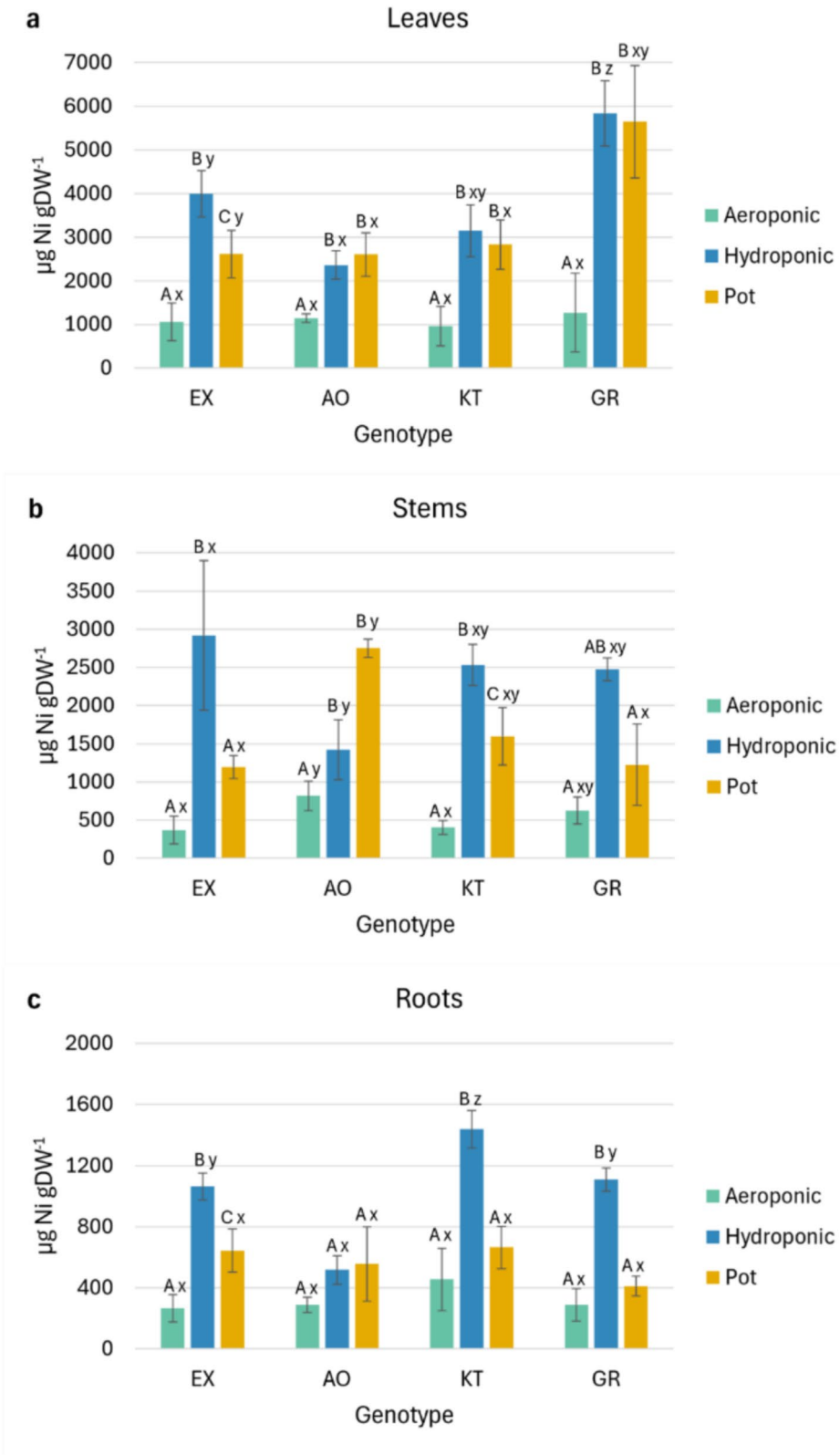
a
Leaves
7000
6000
5000
4000
3000
2000
1000
0
µg Ni gDW-1
B y
C y
B x
A x
B x
B xy
B x
A x
B z
B xy
A x
EX
AO
KT
GR
Genotype
Aeroponic
Hydroponic
Pot
b
Stems
4000
3500
3000
2500
2000
1500
1000
500
0
µg Ni gDW-1
B x
A x
A x
B y
B y
A y
B xy
C xy
A x
AB xy
A x
A xy
EX
AO
KT
GR
Genotype
Aeroponic
Hydroponic
Pot
c
Roots
2000
1600
1200
800
400
0
µg Ni gDW-1
B y
C x
A x
A x
A x
A x
B z
A x
A x
B y
A x
EX
AO
KT
GR
Genotype
Aeroponic
Hydroponic
Pot

◂**Fig. 8** Nickel content (μg g DW^{-1}) in leaves (**a**), stems (**b**) and roots (**c**) of the four genotypes of *Odontarrhena chalcidica* in aeroponic, hydroponic and pot cultivation regimes. Upper case letters and lowercase letters indicate statistically significant differences among cultivation systems within the same genotype and among different genotypes in the same cultivation system and were evaluated by the ANOVA/Kruskal–Wallis tests followed by Tukey HSD/Dunn's tests ($p < 0.05$). Data are given as mean ($n = 4$) ± SD

Overall, the metal distribution followed a similar pattern across all systems and genotypes with higher nickel concentrations in the leaves (960–5840 μg g DW^{-1}), followed by the stems (371–2920 μg g DW^{-1}), and roots (266–1440 μg g DW^{-1}) (Fig. 8). The cultivation system had a strong influence on the efficiency of metal uptake, with individuals grown in hydroponic conditions showing the highest nickel content. An exception was observed for the AO genotype, which displayed the highest nickel concentrations in all three organs when grown in pot (2600, 2752 and 556 μg g DW^{-1} for leaves, stems and roots respectively, Figs. 8a-c). Regarding genotypes comparison, GR emerged as the most efficient accumulator, reaching the highest Ni concentrations in the leaves under both hydroponic and pot conditions (5840 and 5650 μg g DW^{-1}, respectively, Fig. 8a).

The metal translocation from the roots to the aerial parts of each individual was measured by the calculating the Translocation Factor (TF) (Table S7). All individuals displayed a value above 1, with a general average of 7.44. Genotype GR was the more efficient in both hydroponic and pot, having 7.53 and 16.69 respectively. On the contrary, KT genotype had general lower values, on average 4.66 (Table S7).

Discussion

Plant architecture is pivotal in determining biomass yield, as it directly influences light interception, resource allocation, and overall growth efficiency. Biomass is essential in hyperaccumulators for agromining as it directly influences the plant's capacity to absorb and concentrate metals from the soil (Rascio and Navari-Izzo 2011). Key architectural traits such as leaf morphology, stem elongation, and branching patterns are crucial for maximising the photosynthetic surface while minimising self-shading, thereby supporting sustained growth and metal uptake.

The observed results showed apparent architectural dissimilarities among the four analysed *Odontarrhena chalcidica* genotypes collected from different Greek sites at varying altitudes, which appear closely related to their potential for biomass production. Genotypes from lower similar altitudes, GR (615 m a.s.l.), EX (675 m a.s.l.), and AO (650 m a.s.l.), all from West Macedonia, exhibited an upright growth form, in particular EX and GR were characterized by elongated main stems (on average 352.4 mm and 319.5 mm, respectively) (Fig. 4b). This morphology likely results from vegetative competition in environments with higher temperatures and reduced water availability (Lazoglou and Serraos 2021; Milla and Reich 2011). These climatic conditions also favoured the development of smaller, thinner leaves (Wright et al. 2017), a trait particularly evident in AO (Fig. 6). In contrast, the KT genotype, collected from a high-altitude site in Epirus (1683 m a.s.l.), displayed a cushion-like habit, with shorter and sturdier stems (average length of the main stem 198.0 mm and plant height 110.54 mm, Figs. 4b, d) and circular leaves (circularity score 0.75 vs. about 0.5 in the others, Fig. 6). This morphology likely reflects adaptations to mountain conditions such as lower temperatures, winds, higher solar radiation, and increased precipitation (Duruflé et al. 2019), in agreement with previous studies showing the strong influence of environmental pressures on plant morphology (Gratani 2014; Xue et al. 2019). The distinct leaf shapes and growth forms reinforce the hypothesis that natural selection, rather than simple phenotypic plasticity, plays a pivotal role in shaping these architectural traits (Tsukaya 2018). Overall, these observations strengthen the connection between plant architecture and biomass yield, underscoring how morphological adaptations to specific environments can influence productivity potential. Particularly in hyperaccumulator species, an increase in biomass can enhance the plant's capacity for metal uptake, thus amplifying its effectiveness in metal extraction processes.

Plants were grown in three different cultivation systems, each of them showed specific advantages. The growth of plants in pots by using serpentine soil, provided an environment that closely resembled *O. chalcidica* natural habitat, particularly in terms of soil chemical composition and mechanical resistance

to root development. In contrast, the hydroponic system allowed full control over nutrients and metal concentrations (Son et al. 2020), ensuring identical conditions for all individuals. Moreover, with roots continuously immersed in the nutrient solution, drought stress was eliminated. This system also avoids exposure to the pathogens and to the unsuitable physical and chemical properties typical of the soil (Corrêa et al. 2008). The aeroponic system offers an additional advantage to the hydroponics by providing enhanced root aeration and by eliminating the mechanical resistance encountered in soil or water flow (Li et al. 2018; Min et al. 2023).

Plants in the three cultivation systems were exposed to relatively similar levels of bioavailable nickel (Table S1). Although DTPA-extractable Ni in soil (average 5.90 ± 0.96 mg L^{-1}) was higher than the Ni levels in nutrient solutions (average of 1.42 mg L^{-1}), it is still possible to suggests that the experimental hydroponic and aeroponic setups effectively provides a consistent basis for evaluating differences in plant responses across systems. The present data showed the hydroponic system as the best performing both for leaves biomass production (on average EX 5.67 g DW; GR 6.97 g DW; AO 2.06 g DW; KT 5.37 g DW, Fig. 7A) and nickel accumulation in leaves (on average EX 3993.69 µg g DW^{-1}; GR 5838.86 µg g DW^{-1}; AO 2362.02 µg g DW^{-1}; KT 3148.73 µg g DW^{-1}) (Fig. 8a). On the other hand, the other analyzed morphological and physiological plant traits (plant architecture, Fig. 4; specific leaf area, Table S2; stomata and trichome densities, Tables S2 and S3; photosynthetic parameters, Table S4; photosynthetic pigments, Table S5) did not highlight significant differences among cultivation regimes. High biomass production in hydroponics may be attributed to the optimal conditions provided by the nutrient solution and the growth environment. Since the same nutrient solution and growing conditions were also used for aeroponic cultivation, leading to a lower plant biomass (Fig. 7), the hydroponic system likely reduced root-level temperature stress. In contrast, potential stress in the aeroponic system may have affected metal uptake from the nutrient solution, which was comparable to the bioavailable Ni present in the pot soil (on average 1.42 mg L^{-1} in aeroponic and hydroponic; average DTPA extractable Ni 5.90 mg L^{-1} in soil, Table S1). These results demonstrate the potential of hydroponic systems for cultivating *O. chalcidica* in future research and breeding. By controlling environmental factors and nutrient solutions, stable growth and plant health are ensured. Developing speed-breeding protocols (Chaudhary and Sandhu 2024) in hydroponics would be beneficial, as most plant traits remain unaffected by the system. On the other hand, it is important to consider that controlled systems (i.e. glasshouse or growth chambers) simplify plant environments compared to field conditions (Poorter et al. 2016). Therefore, also in the case of *O. chalcidica*, the observed results may not be directly transferable to field performance.

Neither stomatal (adaxial and abaxial surfaces; Table S3) nor trichome (adaxial and abaxial surfaces; Table S4) density varied among the four *O. chalcidica* genotypes or across the aeroponic, hydroponic, and pot cultivation systems. Previous studies have suggested that environmental factors can influence these densities (Casson and Gray 2008; Wang et al. 2021). However, as all cultivation systems in this study were maintained under identical conditions within the same greenhouse, we can conclude that the cultivation regime did not affect these traits. This suggests that both stomata and trichome densities are primarily genetically controlled and exhibit minimal phenotypic plasticity in response to cultivation conditions. Such stability is advantageous for comparative phenotyping, as stomatal and trichome counts can be reliably compared across different cultivation systems without introducing system-specific bias. Furthermore, this constancy implies that these traits maintain a consistent gas-exchange potential across systems (Lawson and Leakey 2024).

Odontarrhena chalcidica exhibited stable physiological performance across different cultivation systems, as shown by photosynthetic parameters (assimilation rate, transpiration rate and stomatal conductance, Table S5) and photosynthetic pigment contents chlorophyll a, chlorophyll b and carotenoids, Table S6), suggesting the overall health of the individuals (Duruflé et al. 2019; Xue et al. 2024). Specifically, the measured average stomatal conductance (GasEx gsw, 0.700 mol H_2O m^{-2} s^{-1}, Table S4) and the observed average assimilation and transpiration rates (GasEx A, 21.688 µmol CO_2 m^{-2} s^{-1}; GasEx E, 0.011 mol H_2O m^{-2} s^{-1}; Table S5) indicated efficient stomatal regulation and active gas exchange across genotypes. These physiological parameters showed no significant variation attributable to cultivation

conditions, supporting the hypothesis that *O. chalcidica* maintains its photosynthetic efficiency under different agronomic contexts. Although the present study evaluated responses across cultivation systems, the findings align with those reported by Scartazza et al. (2022), who observed increased CO_2 assimilation rates in *O. chalcidica* in response to nickel treatment. Both studies agree in highlighting the physiological resilience of this species, supporting the idea that it responds positively to Ni exposure by enhancing its photosynthetic performance. Overall, the stability of physiological traits may serve as a prerequisite for more accurate assessment of the influence of morphological features on improving the agromining yield efficiency.

The concentration of photosynthetic pigments was stable in all cultivation system and genotype, with average values of chlorophyll a (29.16 mg g FW^{-1}), chlorophyll b (9.56 mg g FW^{-1}), and carotenoids (8.3 mg g FW^{-1}) (Table S6). This consistency suggests that the photosynthetic apparatus of the species was well preserved regardless of the adopted growing system, reflecting a robust capacity to maintain light-harvesting and photoprotective functions (Simkin et al. 2022).

In plants, metal ions are absorbed by low-affinity transport systems at the root level, i.e., ZIP (ZRT/IRT-like Protein) family (Deng et al. 2018; Yusuf et al. 2011). Once it enters the cell, the metal has two alternative pathways. The first less common is to be sequestered by the root vacuoles. The second option is the chelation of the ions by organic compounds, e.g., histidine (Robinson et al. 2003), within the rhizodermis, to be then radially transported to the pericycle via symplast. Once the compounds reach the xylem vessels, Ni moves up to the shoots through the xylem flow targeting the leaves. The metal is then sequestrated and stored in the leaf vacuoles, usually chelated by carboxyl acids (Deng et al. 2018; van der Pas and Ingle 2019). This metal flow leads to a gradient of concentration of Ni from root to leaves.

Present data on leaves and roots Ni concentrations (Figs. 8a-c) confirmed that *O. chalcidica* is an effective Ni-hyperaccumulator due to its ability to absorb Ni from the nutrient solution. In fact, all genotypes displayed a Translocation Factor (TF) much higher than 1, indicating an active uptake and translocation of the metal from the nutrient solution, through the roots, followed by accumulation in the leaves (average TF for each genotype: EX 6.18; GR 10.31; AO 8.61; KT 4.66, Table S7).

Metal distribution results revealed a clear influence of the genotypes' origins on their nickel accumulation patterns. GR plants, originated from fluvioglacial sediments with variable Ni availability, exhibited the highest TF (16.69) of all in the pot system (Table S7). This may suggest an adaptive response of GR by promoting enhanced Ni translocation under fluctuating conditions. In contrast, genotypes EX, AO, and KT, sourced from ultramafic soils characterized by constantly high Ni levels, demonstrated lower TF values (Table S7) indicating a more conservative approach to internal metal regulation, likely due to their regular exposure to elevated Ni concentrations. The comparison between genotypes endemic from ultramafic sites (EX, AO and KT) and GR from non-ultramafic environment suggests that the latter may lack tightly regulated mechanisms for metal homeostasis to withstand high metal concentration (Meindl et al. 2014). As a result, it can accumulate more Ni when exposed. These findings highlight the significant role of ecological context in shaping metal transport mechanisms and efficiency across different genotypes. Genotypic variations in metal accumulation could also originate from differences in metal transporter gene sequences, as observed in *Noccaea caerulescens,* a Zn and Cd hyperaccumulator also belonging to the Brassicaceae family (Plaza et al. 2007).

The proven ability of *O. chalcidica* to act as an effective Ni-hyperaccumulator makes it well-suited for agromining in the Mediterranean region, a prospect particularly relevant in the current economic context. However, a key question remains: which genotype is the most suitable for this purpose?

Agromining is a complex process that includes harvesting, where only a portion of the plant, typically the above-ground biomass that reaches a certain height depending on the used harvesting machinery, is employed for metal extraction. Any metal concentration or plant development below this limit can be excluded from economic consideration. Therefore, when selecting a potential population for agromining, traits related to the stems and leaves must be prioritised. According to the results from the study, the AO genotype appeared less suitable for agromining, due to its average stem height which seems incompatible with mechanical harvesting (Fig. 4d). Similarly, while the KT genotype showed promising biomass

and metal accumulation, its prostrate habit may lead to biomass loss and reduced production potential. On the other hand, EX and GR appeared more suitable for agromining (Fig. S1), showing the highest average shoots biomass (Fig. 7) and shoots Ni content (Fig. 8). However, field trials are needed to validate their viability and full potential.

Conclusion

The present study revealed substantial phenotypic variability among of four different genotypes of *Odontarrhena chalcidica*, while demonstrating consistency across cultivation system, supporting hydroponics and aeroponics as reliable growing methods for future phenotyping studies. However, biomass yield, metal uptake, and accumulation differed significantly among regimes, with hydroponics emerging as the most favourable for plant performance. Comparisons across systems offer insights into potential field behaviour, crucial for advancing agromining strategies. Among pot-grown plants, shoot biomass and Ni content were similar across genotypes, but plant architecture pointed to GR and EX as promising candidates for agromining, pending field validation. To strengthen these findings, future studies should include a greater number of genotypes per population to take into consideration intrapopulation phenotypic variability.

Future research integrating molecular biology approaches could help identify key genetic traits responsible for metal uptake and biomass optimization, enabling the selection and enhancement of most efficient genotypes. Moreover, speed breeding techniques could accelerate the development of optimised cultivars with enhanced biomass yield and metal extraction capacity, making agromining a more viable and efficient strategy.

Acknowledgements We wish to thank Professors Claudio Ciavatta and Luigi Manfrini (Department of Agriculture and Food Science, University of Bologna, Italy), for allowing the use of greenhouse and of the Li-Cor instrumentation.

Author contributions Mirko Salinitro and Benedetta Montanarini contributed to the study's conception, design, and material preparation. Benedetta Montanarini and Mirko Salinitro performed data collection. Benedetta Montanarini, Mirko Salinitro and Stefania Monari performed analyses. Maria Roberta Randi and Davide Cavalletti provided support for the ESEM measurements. Annalisa Tassoni and Guillaume Echevarria provided the resources and supervised the study. Benedetta Montanarini wrote the draft of the manuscript, and Annalisa Tassoni, Guillaume Echevarria, and Mirko Salinitro revised and edited the final version.

Funding Open access funding provided by Alma Mater Studiorum - Università di Bologna within the CRUI-CARE Agreement. This work was supported by a PhD fellowship awarded to Benedetta Montanarini under the National Recovery and Resilience Plan (PNRR) – Mission 4, Component 2, Investment 3.3, co-funded by the European Union – Next GenerationEU (D.D. 117 02/03/2022), and by the company ECONICK SAS (Lunéville, France).

Data availability The datasets generated during and/or analysed during the current study are available from the corresponding author on reasonable request.

Declarations

Conflict of interest The authors declare that they have no known competing financial interests or personal relationships that could have appeared to influence the work reported in this paper.

References

Assunção AGL, Schat H, Aarts MGM (2003) *Thlaspi caerulescens*, an attractive model species to study heavy metal hyperaccumulation in plants. New Phytol 159:351–360. https://doi.org/10.1046/j.1469-8137.2003.00820.x

Baker AJM (1981) Accumulators and excluders: strategies in the response of plants to heavy metals. J Plant Nutr 3:643–665. https://doi.org/10.1080/01904168109362867

Baker AJM, Brooks RR (1989) Terrestrial higher plants which hyperaccumulate metallic elements: a review of their distribution, ecology and phytochemistry. Biorecovery 1:81–126

Bani A, Álvarez-López V, Prieto-Fernández A, Miho L, Shahu E, Echevarria G, Kidd P (2024) Designing cropping systems for nickel agromining on ultramafic land in Albania.

Ecol Res 39(6):909–926. https://doi.org/10.1111/1440-1703.12525
Bettarini I, Gonnelli C, Selvi F, Coppi A, Pazzagli L, Colzi I (2021) Diversity of Ni growth response and accumulation in Central-Eastern Mediterranean *Odontarrhena* (Brassicaceae) populations on and off serpentine sites. Environ Exp Bot 186:104455. https://doi.org/10.1016/j.envexpbot.2021.104455
Burkhard LP (2021) Evaluation of published bioconcentration factor (BCF) and bioaccumulation factor (BAF) data for per- and polyfluoroalkyl substances across aquatic species. Environ Toxicol Chem 40:1530–1543. https://doi.org/10.1002/etc.5010
Casson S, Gray JE (2008) Influence of environmental factors on stomatal development. New Phytol 178:9–23. https://doi.org/10.1111/j.1469-8137.2007.02351.x
Cecchi L, Bettarini I, Colzi I, Coppi A, Echevarria G, Pazzagli L, Bani A, Gonnelli C, Selvi F (2018) The genus *Odontarrhena* (Brassicaceae) in Albania: taxonomy and nickel accumulation in a critical group of metallophytes from a major serpentine hot-spot. Phytotaxa. https://doi.org/10.11646/phytotaxa.351.1.1
Cecchi L, Španiel S, Bianchi E, Coppi A, Gonnelli C, Selvi F (2020) *Odontarrhena stridii* (Brassicaceae), a new nickel-hyperaccumulating species from mainland Greece. Plant Syst Evol 306:69. https://doi.org/10.1007/s00606-020-01687-3
Chaney RL, Baklanov IA (2017) Chapter five - Phytoremediation and phytomining: status and promise. Adv Bot Res 83:189–221. https://doi.org/10.1016/bs.abr.2016.12.006
Chaudhary N, Sandhu R (2024) A comprehensive review on speed breeding methods and applications. Euphytica 220:42. https://doi.org/10.1007/s10681-024-03300-x
Corrêa RM, Pinto JEBP, Pinto CABP, Faquin V, Reis ÉS, Monteiro AB, Dyer WE (2008) A comparison of potato seed tuber yields in beds, pots and hydroponic systems. Sci Hort 116:17–20. https://doi.org/10.1016/j.scienta.2007.10.031
Corzo Remigio A, Chaney RL, Baker AJM, Edraki M, Erskine PD, Echevarria G, van der Ent A (2020) Phytoextraction of high value elements and contaminants from mining and mineral wastes: opportunities and limitations. Plant Soil 449:11–37. https://doi.org/10.1007/s11104-020-04487-3
Deng THB, van der Ent A, Tang YT, Sterckeman T, Echevarria G, Morel JL, Qiu RL (2018) Nickel hyperaccumulation mechanisms: a review on the current state of knowledge. Plant Soil 423:1–11. https://doi.org/10.1007/s11104-017-3539-8
Dinno A (2024) Dunn's test of multiple comparisons using rank sums. R package version 1.3.6. https://CRAN.R-project.org/package=dunn.test. Accessed 5 Feb 2024
Duruflé H, Ranocha P, Mbadinga Mbadinga DL, Déjean S, Bonhomme M, San Clemente H, Viudes S, Eljebbawi A, Delorme-Hinoux V, Sáez-Vásquez J, Reichheld J-P, Escaravage N, Burrus M, Dunand C (2019) Phenotypic trait variation as a response to altitude-related constraints in *Arabidopsis* populations. Front Plant Sci 10:430. https://doi.org/10.3389/fpls.2019.00430
Fox J, Weisberg S (2019) An R companion to applied regression, 3rd edn. Sage, Thousand Oaks, CA, USA. https://www.john-fox.ca/Companion/. Accessed 10 Jan 2024
Genchi G, Carocci A, Lauria G, Sinicropi MS, Catalano A (2020) Nickel: human health and environmental toxicology. Int J Environ Res Public Health 17:679. https://doi.org/10.3390/ijerph17030679
Gratani L (2014) Plant phenotypic plasticity in response to environmental factors. Adv Bot 2014:208747. https://doi.org/10.1155/2014/208747
ImageJ (n.d.) Image processing and analysis in java. https://imagej.net/ij/index.html. Accessed 4 Mar 2024
Jaffré T, Brooks RR, Lee J, Reeves RD (1976) *Sebertia acuminata:* a hyperaccumulator of nickel from New Caledonia. Science 193:579–580. https://doi.org/10.1126/science.193.4253.579
Kidd PS, Bani A, Benizri E, Gonnelli C, Hazotte C, Kisser J, Konstantinou M, Kuppens T, Kyrkas D, Laubie B, Malina R, Morel J-L, Olcay H, Pardo T, Pons M-N, Prieto-Fernández Á, Puschenreiter M, Quintela-Sabarís C, Ridard C, Rodríguez-Garrido B, Rosenkranz T, Rozpądek P, Saad R, Selvi F, Simonnot M-O, Tognacchini A, Turnau K, Ważny R, Witters N, Echevarria G (2018) Developing sustainable agromining systems in agricultural ultramafic soils for nickel recovery. Front Environ Sci 6:44. https://doi.org/10.3389/fenvs.2018.00044
Krzciuk K, Gałuszka A (2015) Prospecting for hyperaccumulators of trace elements: a review. Crit Rev Biotech 35:522–532. https://doi.org/10.3109/07388551.2014.922525
Lawson T, Leakey ADB (2024) Stomata: custodians of leaf gaseous exchange. J Exp Bot 75:6677–6682. https://doi.org/10.1093/jxb/erae425
Lazoglou M, Serraos K (2021) Climate change adaptation through spatial planning: the case study of the region of Western Macedonia. IOP Conf Ser: Earth Environ Sci 899:012021. https://doi.org/10.1088/1755-1315/899/1/012021
Li Q, Li X, Tang B, Gu M (2018) Growth responses and root characteristics of lettuce grown in aeroponics, hydroponics, and substrate culture. Horticulturae 4:35. https://doi.org/10.3390/horticulturae4040035
Lindsay WL, Norvell WA (1978) Development of a DTPA soil test for zinc, iron, manganese, and copper. Soil Sci Soc Am J 42:421–428. https://doi.org/10.2136/sssaj1978.03615995004200030009x
Mankins W, Lamb S (1990) Nickel and nickel alloys. In: AH Committee (ed) Properties and selection: non-ferrous alloys and special-purpose materials ASM Handbook. ASM International, pp. 428–445. https://doi.org/10.31399/asm.hb.v02.a0001072.
Meindl GA, Bain DJ, Ashman TL (2014) Nickel accumulation in leaves, floral organs and rewards varies by serpentine soil affinity. AoB Plants 6:plu036. https://doi.org/10.1093/aobpla/plu036
Meshram P, Abhilash, and Pandey BD (2019) Advanced review on extraction of nickel from primary and secondary sources. Miner Process Extr Metall Rev 40:157–193. https://doi.org/10.1080/08827508.2018.1514300.
Milla R, Reich PB (2011) Multi-trait interactions, not phylogeny, fine-tune leaf size reduction with increasing altitude. Ann Bot 107:455–465. https://doi.org/10.1093/aob/mcq261

Min A, Nguyen N, Howatt L, Tavares M, Seo J (2023) Aeroponic systems design: considerations and challenges. J Agric Eng 54:1387. https://doi.org/10.4081/jae.2022.1387

Mistry M, Gediga J, Boonzaier S (2016) Life cycle assessment of nickel products. Int J Life Cycle Assess 21:1559–1572. https://doi.org/10.1007/s11367-016-1085-x

Pachura P, Ociepa-Kubicka A, Skowron-Grabowska B (2016) Assessment of the availability of heavy metals to plants based on the translocation index and the bioaccumulation factor. Desalin Water Treat 57:1469–1477. https://doi.org/10.1080/19443994.2015.1017330

Paulikas D, Katona S, Ilves E, Ali SH (2020) Life cycle climate change impacts of producing battery metals from land ores versus deep-sea polymetallic nodules. J Clean Prod 275:123822. https://doi.org/10.1016/j.jclepro.2020.123822

Plaza S, Tearall KL, Zhao FJ, Buchner P, McGrath SP, Hawkesford MJ (2007) Expression and functional analysis of metal transporter genes in two contrasting ecotypes of the hyperaccumulator *Thlaspi caerulescens*. J Exp Bot 58:1717–1728. https://doi.org/10.1093/jxb/erm025

Poorter H, Fiorani F, Pieruschka R, Wojciechowski T, van der Putten WH, Kleyer M, Schurr U, Postma J (2016) Pampered inside, pestered outside? Differences and similarities between plants growing in controlled conditions and in the field. New Phytol 212:838–855. https://doi.org/10.1111/nph.14243

QGIS Development Team (2022) QGIS Geographic Information System, version 3.34. Open Source Geospatial Foundation Project. https://qgis.org. Accessed 8 Feb 2024

R Core Team (2023) R: a language and environment for statistical computing, version 4.3.2. R Foundation for Statistical Computing, Vienna, Austria. https://www.R-project.org. Accessed 10 Jan 2024

Radwan DEM, Fayez KA, Mahmoud SY, Hamad A, Lu G (2007) Physiological and metabolic changes of *Cucurbita pepo* leaves in response to zucchini yellow mosaic virus (ZYMV) infection and salicylic acid treatments. Plant Physiol Biochem 45:480–489. https://doi.org/10.1016/j.plaphy.2007.03.002

Rascio N, Navari-Izzo F (2011) Heavy metal hyperaccumulating plants: how and why do they do it? And what makes them so interesting? Plant Sci 180:169–181. https://doi.org/10.1016/j.plantsci.2010.08.016

Reeves RD, Baker AJM, Jaffré T, Erskine PD, Echevarria G, van der Ent A (2018) A global database for plants that hyperaccumulate metal and metalloid trace elements. New Phytol 218:407–411. https://doi.org/10.1111/nph.14907

Robinson BH, Lombi E, Zhao FJ, McGrath SP (2003) Uptake and distribution of nickel and other metals in the hyperaccumulator *Berkheya coddii*. New Phytol 158:279–285. https://doi.org/10.1046/j.1469-8137.2003.00743.x

Rosenkranz T, Hipfinger C, Ridard C, Puschenreiter M (2019) A nickel phytomining field trial using *Odontarrhena chalcidica* and *Noccaea goesingensis* on an Austrian serpentine soil. J Environ Manage 242:522–528. https://doi.org/10.1016/j.jenvman.2019.04.073

Scartazza A, Di Baccio D, Mariotti L, Bettarini I, Selvi F, Pazzagli L, Colzi I, Gonnelli C (2022) Photosynthesizing while hyperaccumulating nickel: insights from the genus *Odontarrhena* (Brassicaceae). Plant Physiol Biochem 176:9–20. https://doi.org/10.1016/j.plaphy.2022.02.009

Schindelin J, Arganda-Carreras I, Frise E, Kaynig V, Longair M, Pietzsch T, Preibisch S, Rueden C, Saalfeld S, Schmid B, Tinevez JY, White DJ, Hartenstein V, Eliceiri K, Tomancak P, Cardona A (2012) Fiji: an open-source platform for biological-image analysis. Nat Methods 9:676–682. https://doi.org/10.1038/nmeth.2019

Schneider CA, Rasband WS, Eliceiri KW (2012) NIH Image to ImageJ: 25 years of image analysis. Nature Methods 9(7):671–675. https://doi.org/10.1038/nmeth.2089

Simkin AJ, Kapoor L, Doss CGP, Hofmann TA, Lawson T, Ramamoorthy S (2022) The role of photosynthesis related pigments in light harvesting, photoprotection and enhancement of photosynthetic yield in planta. Photosynth Res 152:23–42. https://doi.org/10.1007/s11120-021-00892-6

Son JE, Kim HJ, Ahn TI (2020) Hydroponic systems. In: T Kozai, G Niu, M Takagaki (eds) Plant Factory: an indoor vertical farming system for efficient quality food production. 2nd edn. Academic Press, Cambridge, MA, pp. 273–283. https://doi.org/10.1016/B978-0-12-816691-8.00020-0.

Tsukaya H (2018) A consideration of leaf shape evolution in the context of the primary function of the leaf as a photosynthetic organ. In: WW Adams III, I Terashima (eds) The leaf: a platform for performing photosynthesis. Springer International Publishing, Cham, pp. 1–26. https://doi.org/10.1007/978-3-319-93594-2_1.

van der Pas L, Ingle R (2019) Towards an understanding of the molecular basis of nickel hyperaccumulation in plants. Plants 8:11. https://doi.org/10.3390/plants8010011

van der Ent A, Echevarria G, Baker AJM, Morel JL (2018) Agromining: farming for metals. Extracting unconventional resources using plants. Springer International Publishing, Cham, Switzerland

van der Ent A, Malaisse F, Erskine PD, Mesjasz-Przybyłowicz J, Przybyłowicz WJ, Barnabas AD, Sośnicka M, Harris HH (2019) Abnormal concentrations of Cu–Co in *Haumaniastrum katangense*, *Haumaniastrum robertii* and *Aeolanthus biformifolius*: contamination or hyperaccumulation? Metallomics 11:586–596. https://doi.org/10.1039/c8mt00300a

Wang X, Shen C, Meng P, Tan G, Lv L (2021) Analysis and review of trichomes in plants. BMC Plant Biol 21:70. https://doi.org/10.1186/s12870-021-02840-x

Winjobi O, Kelly JC, Dai Q (2022) Life-cycle analysis, by global region, of automotive lithium-ion nickel manganese cobalt batteries of varying nickel content. Sust Mater Technol 32:e00415. https://doi.org/10.1016/j.susmat.2022.e00415

Wright IJ, Dong N, Maire V, Prentice IC, Westoby M, Díaz S, Gallagher RV, Jacobs BF, Kooyman R, Law EA, Leishman MR, Niinemets Ü, Reich PB, Sack L, Villar R, Wang H, Wilf P (2017) Global climatic drivers of leaf size. Science 357:917–921. https://doi.org/10.1126/science.aal4760

Xue B, Sartori P, Leibler S (2019) Environment-to-phenotype mapping and adaptation strategies in varying environments. Proc Natl Acad Sci U S A 116:13847–13855. https://doi.org/10.1073/pnas.1903232116

Xue R, Zuo W, Zheng Z, Han Q, Shi J, Zhang Y, Qiu J, Wang S, Zhu Y, Cao W, Zhang X (2024) Interpreting controls of stomatal conductance across different vegetation types via machine learning. Water 16:2251. https://doi.org/10.3390/w16162251

Yusuf M, Fariduddin Q, Hayat S, Ahmad A (2011) Nickel: an overview of uptake, essentiality and toxicity in plants. Bull Environ Contam Toxicol 86:1–17. https://doi.org/10.1007/s00128-010-0171-1